Synthesis, Characterization, and Substitution Chemistry of $[Bu_4N]_2[W_6Cl_8(OSO_2CF_3)_6]$. A Versatile Precursor for Axially Substituted Clusters Containing the $\{W_6Cl_8\}^{4+}$ Core

Charles S. Weinert, Charlotte L. Stern, and Duward F. Shriver*

Department of Chemistry, Northwestern University, Evanston, Illinois 60208

Received July 2, 1999

The new cluster $[Bu_4N]_2[W_6Cl_8(OSO_2CF_3)_6]$ (**1**) has been prepared and structurally characterized. This material is an effective precursor for the generation of cluster ions with the general formula $[W_6Cl_8L_6]^n$ ($L = Cl^-$, Br^-, I^-, NCS^-, NCO^-, $NCSe^-$, and $O{=}PPh_3$; $n = 2-$ or $4+$). The last three clusters are new. The products have been characterized by IR spectroscopy, NMR spectroscopy, and FAB mass spectrometry. In addition to **1**, the products $[Bu_4N]_2[W_6Cl_8(NCS)_6]$ (**5**) and $[Bu_4N]_2[W_6Cl_8(NCO)_6]$ (**7**) were structurally characterized. Crystal data for **1**: space group, $P2_1/c$ (No. 14); $a = 11.116(5)$ Å; $b = 27.952(1)$ Å; $c = 24.516(1)$ Å; $\beta = 95.182(9)°$; $V = 7586.3(5)$ Å^3; $Z = 4$. Crystal data for **5**: space group, $P2_1/n$ (No. 14); $a = 11.3323(9)$ Å; $b = 12.3404(9)$ Å; $c = 44.583(3)$ Å; $\beta = 97.089(1)°$; $V = 6187.1(7)$ Å^3; $Z = 4$. Crystal data for **7**: space group, $P\bar{1}$ (No. 2); $a = 11.8009(8)$ Å; $b = 11.9332(8)$ Å; $c = 11.9522(8)$ Å; $\alpha = 77.904(1)°$; $\beta = 95.182(9)°$; $\gamma = 62.574(1)°$; $V = 1450.5(2)$ Å^3; $Z = 1$.

Introduction

The chemistry of early d-block transition metal clusters $[M_6X_8Y_6]^{n-}$ and $[M_6X_{12}Y_6]^{n-}$ exhibit interesting electrochemical and photophysical properties.[1−11] Interest in group 6 metal clusters and their coordination chemistry has resulted due to their relation to the superconducting Chevrel phases.[10,12−16] These clusters consist of a substitution-inert inner core $\{M_6X_8\}^{n+}$ (M = Mo, W) or $\{M_6X_{12}\}^{n+}$ (M = Nb, Ta) surrounded by six axial ligands. The axial ligands are somewhat more labile than the core ligands, and their substitution chemistry has been a focus of recent research.[1] The substitutional lability of the axial positions can be enhanced by the introduction of weakly coordinated ligands such as acetonitrile,[17] trifluoroacetate,[18] nitrate,[19−21] tetrafluoroborate,[19,22−25] alcohols,[26] and triflate (trifluoromethanesulfonate, OSO_2CF_3)[27−30] at these positions. While the substitution chemistry of the clusters $[Mo_6X_8Y_6]^{n-}$ has been studied in great detail, that of the clusters $[W_6X_8Y_6]^{n-}$ and $[M_6X_{12}Y_6]^{n-}$ (M = Nb, Ta) is less developed.[1]

The triflate clusters $[Mo_6Cl_8(OSO_2CF_3)_6]^{2-}$,[27] $[Ta_6Cl_{12}(OSO_2CF_3)_6]^{2-}$,[29] and $[Nb_6Cl_{12}(OSO_2CF_3)_6]^{3-}$ [30] have been prepared and characterized, and their substitution chemistry has been explored.[28,31] The lightly coordinated tungsten cluster $[W_6I_8(OSO_2CF_3)_6]^{2-}$ serves as a useful precursor for substituted species containing the $\{W_6I_8\}^{4+}$ core.[32] We now report the synthesis, structure, and substitution chemistry of the cluster $[W_6Cl_8(OSO_2CF_3)_6]^{2-}$, which is easily prepared from the all-chloro cluster $[W_6Cl_8Cl_6]^{2-}$, is soluble in noncoordinating solvents such as CH_2Cl_2, and undergoes facile axial ligand substitution to yield

(1) Prokopuk, N.; Shriver, D. F. *Adv. Inorg. Chem.* **1999**, *46*, 1−49.
(2) Zietlow, T. C.; Hopkins, M. D.; Gray, H. B. *J. Solid State Chem.* **1985**, *57*, 112−119.
(3) Jackson, J. A.; Turro, C.; Newsham, M. D.; Nocera, D. G. *J. Phys. Chem.* **1990**, *94*, 4500−4507.
(4) Nocera, D. G.; Gray, H. B. *J. Am. Chem. Soc.* **1984**, *106*, 824−825.
(5) Maverick, A. W.; Gray, H. B. *J. Am. Chem. Soc.* **1981**, *103*, 1298−1300.
(6) Maverick, A. W.; Najdzionek, J. S.; MacKenzie, D.; Nocera, D. G.; Gray, H. B. *J. Am. Chem. Soc.* **1983**, *105*, 1878−1882.
(7) Mussell, R. D.; Nocera, D. G. *Inorg. Chem.* **1990**, *29*, 3711−3717.
(8) Zietlow, T. C.; Nocera, D. G.; Gray, H. B. *Inorg. Chem.* **1986**, *25*, 1351−1353.
(9) Zietlow, T. C.; Schaefer, W. P.; Sadeghi, B.; Hua, N.; Gray, H. B. *Inorg. Chem.* **1986**, *25*, 2195−2198.
(10) Saito, T.; Yoshikawa, A.; Yamagata, T.; Imoto, H.; Unoura, K. *Inorg. Chem.* **1989**, *28*, 3588−3592.
(11) Kepert, D. L.; Marshall, R. E.; Taylor, D. *J. Chem. Soc., Dalton Trans.* **1974**, 506−509.
(12) Ehrlich, G. M.; Warren, C. J.; Vennos, D. A.; Ho, D. M.; Haushalter, R. C.; DiSalvo, F. J. *Inorg. Chem.* **1995**, *34*, 4454−4459.
(13) Xie, X.; McCarley, R. E. *Inorg. Chem.* **1995**, *34*, 6124−6129.
(14) Xie, X.; McCarley, R. E. *Inorg. Chem.* **1996**, *35*, 2713−2714.
(15) Xie, X.; McCarley, R. E. *Inorg. Chem.* **1997**, *36*, 4011−4016.
(16) Zhang, X.; McCarley, R. E. *Inorg. Chem.* **1995**, *34*, 2678−2683.
(17) Ehrlich, G. M.; Warren, C. J.; Haushalter, R. C.; DiSalvo, F. J. *Inorg. Chem.* **1995**, *34*, 4284−4286.
(18) Harder, K.; Preetz, W. *Z. Anorg. Allg. Chem.* **1992**, *612*, 97−100.
(19) Preetz, W.; Bublitz, D.; Schnering, H. G. v.; Sassmannshausen, J. *Z. Anorg. Allg. Chem.* **1994**, *620*, 234−246.
(20) Bublitz, D.; Preetz, W.; Simsek, M. K. *Z. Anorg. Allg. Chem.* **1997**, *623*, 1−7.
(21) Simsek, M. K.; Preetz, W. *Z. Anorg. Allg. Chem.* **1997**, *623*, 515−523.
(22) Harder, K.; Peters, G.; Preetz, W. *Z. Anorg. Allg. Chem.* **1991**, *598*/*599*, 139−149.
(23) Preetz, W.; Harder, K.; Schnering, H. G. v.; Kliche, G.; Peters, K. *J. Alloys Compd.* **1992**, *183*, 413−429.
(24) Bruckner, P.; Peters, G.; Preetz, W. *Z. Anorg. Allg. Chem.* **1993**, *619*, 551−558.
(25) Bruckner, P.; Peters, G.; Preetz, W. *Z. Anorg. Allg. Chem.* **1993**, *619*, 1920−1926.
(26) Basic, I.; Brniceveic, N.; Beck, U.; Simon, A.; McCarley, R. E. *Z. Anorg. Allg. Chem.* **1998**, *624*, 725−732.
(27) Johnston, D. H.; Gaswick, D. C.; Lonergan, M. C.; Stern, C. L.; Shriver, D. F. *Inorg. Chem.* **1992**, *31*, 1869−1873.
(28) Johnston, D. H.; Stern, C. L.; Shriver, D. F. *Inorg. Chem.* **1993**, *32*, 5170−5175.
(29) Kennedy, V. O.; Stern, C. L.; Shriver, D. F. *Inorg. Chem.* **1994**, *33*, 5967−5969.
(30) Prokopuk, N.; Weinert, C. S.; Kennedy, V. O.; Siska, D. P.; Jeon, H. J.; Stern, C. L.; Shriver, D. F. Manuscript in preparation.
(31) Prokopuk, N.; Kennedy, V. O.; Stern, C. L.; Shriver, D. F. *Inorg. Chem.* **1998**, *37*, 5001−5006.
(32) Franolic, J. D.; Long, J. R.; Holm, R. H. *J. Am. Chem. Soc.* **1995**, *117*, 8139−8153.

10.1021/ic990791+ CCC: $19.00
Published on Web 12/18/1999

clusters containing halides and pseudohalides in the axial positions, as well as the neutral ligand triphenylphosphine oxide.

Experimental Section

Instrumentation. IR spectra were obtained using a Bomem MB-100 FTIR spectrometer with 2 cm^{-1} resolution on samples as Nujol mulls sandwiched KBr plates or in solutions using CaF_2 solution cells having a 0.1 mm path length. Mass spectra were obtained at the Nebraska Center for Mass Spectrometry or the Analytical Services Laboratory at Northwestern University. Elemental analyses were performed by Midwest Microlabs. ^{13}C NMR were recorded at 75.4 MHz using a Varian VXR-300 spectrometer and were internally referenced to solvent resonances. ^{31}P NMR spectra were recorded at 121 MHz using a Gemini 300 spectrometer and were referenced to external 85% H_3PO_4.

Materials. All manipulations were carried out under an inert atmosphere of nitrogen using standard Schlenk, syringe, and glovebox techniques.[33] The W(II) cluster $(H_3O)_2[W_6Cl_8Cl_6](OH_2)_n$ was prepared by a literature route[34] and was converted to its tetrabutylammonium salt by metathesis with excess tetrabutylammonium chloride in ethanol. The $[Bu_4N]^+$ salt was precipitated and isolated by filtration and dried in vacuo overnight. Bis(triphenylphosphine)iminium ($[PPN]^+$) and benzyltrimethylammonium ($[BzMe_3N]^+$) salts of the cluster were prepared in an analogous manner. All regents were used as received from Aldrich unless otherwise stated. Solvents were dried according to standard procedures and freshly distilled before use.

Synthesis of $[Bu_4N]_2[W_6Cl_8(OSO_2CF_3)_6]$ (1). The cluster $[Bu_4N]_2[W_6Cl_8Cl_6]$ (**2**) (1.66 g, 0.797 mmol) was dissolved in 350 mL of CH_2Cl_2, and the solution was transferred via syringe to a flask containing silver trifluoromethanesulfonate (1.57 g, 6.11 mmol). The resulting slurry was stirred in the absence of light for 4 h. The precipitated AgCl was removed by filtration through a medium-porosity glass frit containing Celite as a filtration aid. The yellow filtrate was concentrated to approximately 20 mL, and 100 mL of diethyl ether was layered onto the CH_2Cl_2, resulting in the formation of bright yellow crystals of **1**. The product was isolated by filtration, was washed with 3 × 10 mL of diethyl ether, and dried in vacuo to yield 1.78 g (81%) of **1**. The product was stored under a N_2 atmosphere. Anal. Calcd for $C_{38}H_{72}Cl_8F_{18}N_2O_{18}S_6W_6$: C, 16.50; H, 2.62; N, 1.01. Found: C, 16.25; H, 2.49; N, 1.03.

Synthesis of $[Bu_4N]_2[W_6Cl_8X_6]$ (X = Cl^- (2), Br^- (3), I^- (4)). A 7-fold excess of the tetrabutylammonium salt of the anion $[Bu_4N]X$ (X = Cl^-, Br^-, or I^-) and **1** (0.100 g, 0.0362 mmol) were weighed in the glovebox, combined, and dissolved in 8 mL of CH_2Cl_2. The solution was stirred for 2 h, concentrated under vacuum to approximately 2 mL, and layered with diethyl ether (5 mL). The resulting solids were isolated by filtration, washed with 3 × 3 mL of diethyl ether, and then dried in vacuo. Yield: for X = Cl^-, 72%; for X = Br^-, 66%; for X = I^-, 85%. Anal. Calcd for $C_{32}H_{72}Br_6Cl_8N_2W_6$ (**3**): C, 16.35; H, 3.09; N, 1.19. Found: C, 16.54; H, 3.18; N, 1.16. Anal. Calcd for $C_{32}H_{72}Cl_8I_6N_2W_6$ (**4**): C, 14.60; H, 2.76; N, 1.06. Found: C, 14.24; H, 2.59; N, 0.97.

Synthesis of $[Bu_4N]_2[W_6Cl_8(NCS)_6]$ (5) and $[Bu_4N]_2[W_6Cl_8(NCSe)_6]$ (6). A solution of KSCN (0.081 g, 0.832 mmol) in 5 mL of methanol was prepared. Compound **1** (0.213 g, 0.0770 mmol) was weighed in the glovebox and dissolved in 3 mL of methanol with stirring. The KSCN solution was added via syringe, resulting in the formation of a brown/yellow precipitate. The mixture was immediately filtered, and the solids were washed with 2 × 5 mL of methanol. The dark brown filtrate was discarded, the precipitate was dissolved in 5 mL of CH_2Cl_2, and the solution was filtered. The filtrate was reduced to approximately 2 mL and then layered with 5 mL of diethyl ether. The resulting lemon-yellow precipitate was isolated by filtration, washed with 2 × 5 mL diethyl ether, and dried in vacuo to yield 0.072 g (42%). Since **1** rapidly decomposes in methanol, this procedure was carried out rapidly to maximize the yield. Cluster **6** was prepared by an analogous procedure, using KNCSe (0.069 g, 0.479 mmol) and **1** (0.168 g, 0.0608 mmol) to yield 0.062 g (41%). Anal. Calcd for $C_{38}H_{72}Cl_8N_8S_6W_6$ (**5**): C, 20.56; H, 3.27; N, 5.05. Found: C, 20.63; H, 3.19; N, 4.89. Anal. Calcd for $C_{38}H_{72}Cl_8N_8Se_6W_6$ (**6**): C, 18.24; H, 2.90; N, 4.48. Found: C, 17.45; H, 2.77; N, 4.39.

Synthesis of $[Bu_4N]_2[W_6Cl_8(NCO)_6]$ (7). A solution of NaNCO (0.028 g, 0.431 mmol) in 8 mL of methanol was prepared. Compound **1** (0.127 g, 0.0459 mmol) was weighed in the glovebox and then dissolved in 2 mL of methanol with stirring. The NaNCO solution was added via syringe, resulting in the formation of a pale yellow precipitate. The solution was immediately filtered, and the precipitate was washed with 2 × 2 mL of methanol. The solids were discarded, and the methanol was removed in vacuo, resulting in a dark yellow oily solid. This material was dissolved in 3 mL of CH_2Cl_2, and the solution was filtered and then layered with 6 mL of diethyl ether. The resulting lemon-yellow solid was isolated by filtration and dried in vacuo to yield 0.036 g (37%). This procedure was carried out rapidly due to the rapid decomposition of **1** in methanol. Anal. Calcd for $C_{38}H_{72}Cl_8N_8O_6W_6$: C, 21.49; H, 3.42; N, 5.28. Found: C, 21.49; H, 3.41; N, 5.27.

Synthesis of $[W_6Cl_8(O{=}PPh_3)_6][OSO_2CF_3]_4$ (8). Compound **1** (0.077 g, 0.0280 mmol) was weighed in the glovebox and dissolved in 8 mL of CH_2Cl_2. Triphenylphosphine oxide (0.032 g, 0.115 mmol) was dissolved in 5 mL of CH_2Cl_2 and was added via syringe to **1**. The solution was stirred for 2 h, and the volume of the solution was then reduced in vacuo to approximately 2 mL. Diethyl ether (5 mL) was layered onto the CH_2Cl_2 solution. The resulting pale yellow solid was isolated by filtration, washed with 3 × 5 mL of diethyl ether, and dried in vacuo to yield 0.054 g (53%). Anal. Calcd for $C_{112}H_{80}Cl_8F_{12}O_{18}P_6S_4W_6$: C, 36.83; H, 2.40. Found: C, 35.76; H, 2.37.

Crystal Structures of $[Bu_4N]_2[W_6Cl_8(OSO_2CF_3)_6]$ (1), $[Bu_4N]_2[W_6Cl_8(NCS)_6]$ (5), and $[Bu_4N]_2[W_6Cl_8(NCO)_6$ (7). Yellow crystals of $[Bu_4N]_2[W_6Cl_8(OSO_2CF_3)_6]$ (**1**), $[Bu_4N]_2[W_6Cl_8(NCS)_6]$ (**5**), and $[Bu_4N]_2[W_6Cl_8(NCO)_6]$ (**7**) were grown by slow diffusion of diethyl ether into a CH_2Cl_2 solution of the cluster. A crystal measuring 0.12 × 0.10 × 0.03 mm (**1**), 0.50 × 0.10 × 0.03 mm (**5**), or 0.09 × 0.10 × 0.01 mm (**7**) was mounted on a glass fiber using Paratone-N oil (Exxon) and was transferred to the N_2 cold stream (−120 °C) of Bruker CCD diffractometer. All measurements were made with graphite-monochromated Mo Kα radiation. A set of 25 reflections was used to determine the cell constants. For **1**, on the basis of the systematic absences of $h\ 0\ l$ ($l = 2n \pm 1$) and $0\ k\ 0$ ($k = 2n \pm 1$) and successful solution and refinement of the structure, the space group was determined to be $P2_1/c$ (No. 14). Data were collected at −120 °C to a maximum 2θ value of 56.8°, in 0.25° oscillations with 20.0 s exposure times. A total of 47 305 reflections were collected of which 18 197 were unique ($R_{int} = 0.078$). The data were corrected for Lorentz and polarization effects. An empirical absorption correction (SADABS-NT) was applied, resulting in transmission factors ranging from 0.29 to 0.81.

For **5**, on the basis of the systematic absences of $h\ 0\ l$ ($h + l = 2n$) and $0\ k\ 0$ ($k = 2n$) and successful solution and refinement of the structure, the space group was determined to be $P2_1/n$ (No. 14). Data were collected at −120 °C to a maximum 2θ value of 56.7°, in 0.30° oscillations with 15.0 s exposure times. A total of 57 230 reflections were collected of which 15 567 were unique ($R_{int} = 0.135$). The data were corrected for Lorentz and polarization effects. An analytical face-indexed absorption correction was applied (Bruker ShelXTL-NT), resulting in transmission factors ranging from 0.0995 to 0.7241.

For **7**, by successful solution and refinement of the structure, the space group was determined to be $P\bar{1}$ (No. 2). Data were collected at −120 °C to a maximum 2θ value of 56.7°, in 0.30° oscillations with 20.0 s exposure times. A total of 13 447 reflections were collected of which 6732 were unique ($R_{int} = 0.049$). The data were corrected for Lorentz and polarization effects. An analytical face-indexed absorption correction was applied (Bruker ShelXTL-NT), resulting in transmission factors ranging from 0.3425 to 0.8978.

All calculations were carried out using the teXsan crystallographic software package (Molecular Structure Corporation).[35] The structures

(33) Shriver, D. F.; Drezdzon, M. A. *The Manipulation of Air Sensitive Compounds*, 2nd ed.; John Wiley & Sons: New York, 1986.
(34) Dorman, W. C.; McCarley, R. E. *Inorg. Chem.* **1974**, *13*, 491−493.
(35) *Texsan, Crystal Structure Analysis Package*; Molecular Structure Corporation: The Woodlands, TX, 1985 and 1992.

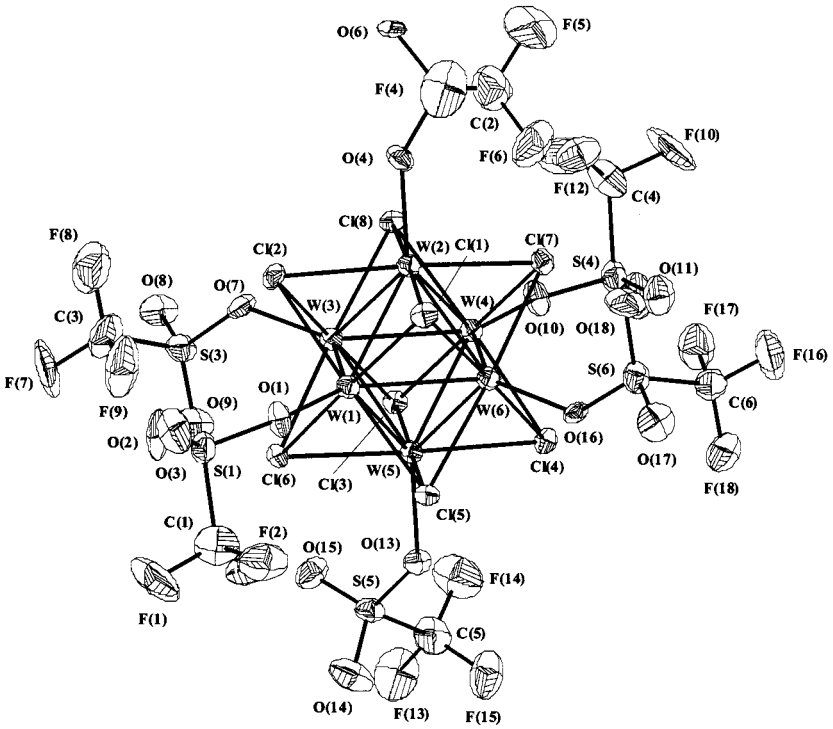

Figure 1. ORTEP diagram of the cluster anion of $[Bu_4N]_2[W_6Cl_8(OSO_2CF_3)_6]$ (**1**). Thermal ellipsoids are drawn at 50% probability.

Table 1. Infrared Spectra and Assignments[a] of $[Bu_4N]_2[W_6Cl_8(OSO_2CF_3)_6]$ (**1**) and $[Bu_4N]_2[Mo_6Cl_8(OSO_2CF_3)_6]$ (**9**) in Nujol Mull and Solid $NaOSO_2CF_3$ (in cm^{-1})

species	$\nu_{as}(SO_3)$[c]	$\nu_s(CF_3)$	$\nu_{as}(CF_3)$	$\nu_s(SO_3)$
$[Bu_4N]_2[W_6Cl_8(OSO_2CF_3)_6]$				
Nujol mull	1346	1237	1160	988
	1196, 1182(sh)			
CH_2Cl_2	1349, 1200	1235	1165	997
$[Bu_4N]_2[Mo_6Cl_8(OSO_2CF_3)_6]$	1343	1234	1162	990
	1199, 1181(sh)			
$NaOSO_2CF_3$[b]	1280	1232	1168	1036

[a] Assignments from Buerger, H.; Burczyk, K.; Blaschette, A. *Montash. Chem.* **1970**, *101*, 102. [b] Miles, M. G.; Doyle, G.; Cooney, R. P.; Tobias, R. S. *Spectrochim. Acta* **1969**, *25*, 1515. [c] This degenerate stretching mode splits upon coordination.

were solved using direct methods[36] and expanded using Fourier techniques.[37] Neutral atom scattering factors were taken from Comer and Waber.[38] Anomalous dispersion effects were included in F_{calc}.[39] The values for $\Delta f'$ and $\Delta f''$ were those of Creagh and McAuley.[40] The values for the mass attenuation coefficients were those of Creagh and Hubbell.[41]

For **1** and **7**, the non-hydrogen atoms were refined anisotropically. Hydrogen atoms were included in idealized positions but not refined. For **5**, atoms on the cluster dianion and the nitrogen atoms of the cations were refined anisotropically, while all other atoms were refined isotropically. Disordered carbon atoms in the cations were refined with group isotropic thermal parameters. Hydrogen atoms were included in idealized positions but not refined on the ordered cation. The final cycle of full-matrix least squares refinement on F^2 was based on 7395 observed reflections and 865 variable parameters and converged (largest parameter shift was 0.015 times its esd) to an R value of 0.043 (R_w = 0.086) for **1**, while for **7** this refinement on F^2 was based on 3425 observed reflections and 298 variable parameters and converged (largest parameter shift was 0.000 times its esd) to an R value of 0.042 (R_w = 0.053). For **5**, this refinement on F^2 was based on 4109 observed reflections and 447 variable parameters and converged (largest parameter shift was 0.01 times its esd) to an R value of 0.057 (R_w = 0.114). The standard deviations of a unit weight were 1.17 (**1**), 1.39 (**5**), and 0.85 (**7**). The weighting schemes were based on counting statistics and, in the case of **1**, included a factor (p = 0.004) to downweight the intense reflections. Plots of $\sum w(|F_o| - |F_c|)^2$ versus $|F_o|$, reflection order in data collection, sin θ/λ, and various classes of indices showed no unusual trends. The maximum and minimum peaks on the final difference Fourier map respectively corresponded to 2.42 and −4.85 $e^-/Å^3$ for **1**, 2.96 and −1.37 $e^-/Å^3$ for **5**, 1.21 and −0.84 $e^-/Å^3$ for **7**. These were in all cases located in the vicinity of the tungsten positions.

Results and Discussion

The triflate cluster $[Bu_4N]_2[W_6Cl_8(OSO_2CF_3)_6]$ (**1**) has been prepared from the all-chloro cluster $[Bu_4N]_2[W_6Cl_8Cl_6]$ (**2**) in high yield by chloride abstraction at all six axial positions. The IR spectrum of **1** in Nujol closely resembles that of $[Bu_4N]_2[Mo_6Cl_8(OSO_2CF_3)_6]$ (**9**) (Table 1).[27] The strong sulfur−oxygen stretching bands provide a method of monitoring the coordination of the triflate ligand to the cluster. The symmetry of the triflate anion is reduced from C_{3v} to C_s, upon coordination to the cluster. This results in the splitting of the degenerate (E-symmetry) asymmetric SO_3 stretch found at 1280 cm^{-1} in $NaOSO_2CF_3$[42] into two bands at 1347 and 1197 cm^{-1} for **1** in a Nujol mull. The symmetric SO_3 stretch in **1** has been lowered

(36) Sheldrick, G. M. SHELXS86. In *Crystallographic Computing 3*; Sheldrick, G. M., Kruger, C., Goddard, R., Eds.; Oxford University Press: Oxford, 1985; pp 175−189.
(37) DIRDIF92: Beurskens, P. T.; Admiral, G.; Beurskens, G.; Bosman, W. P.; Garcia-Granda, S.; Gould, R. O.; Smits, J. M. M.; Smykalla, C. *The DIRDIF program system: Direct methods for difference structure factors*; Technical Report of the Crystallography Laboratory: University of Nijmgegen, The Netherlands, 1992.
(38) Cromer, D. T.; Waber, J. T. *International Tables for X-Ray Crystallography*; The Kynoch Press: Birmingham, England, 1974; Vol. IV.
(39) Ibers, J. A.; Hamilton, W. C. *Acta Crystallogr.* **1964**, *17*, 781.
(40) Creagh, D. C.; McAuley, W. J. *International Tables for X-Ray Crystallography*; Kluwer Academic Publishers: Boston, 1992; Vol. C.
(41) Creagh, D. C.; Hubbell, J. H. *International Tables for X-Ray Crystallography*; Kluwer Academic Publishers: Boston, 1992; Vol. C Table 2.3.4.3, pp 200−206.
(42) Johnston, D. H.; Shriver, D. F. *Inorg. Chem.* **1993**, *32*, 1045−1047.

Table 2. Crystallographic Data for $[Bu_4N]_2[W_6Cl_8(OSO_2CF_3)_6]$ (**1**), $[Bu_4N]_2[W_6Cl_8(NCS)_6]$ (**5**), and $[Bu_4N]_2[W_6Cl_8(NCO)_6]$ (**7**)

	1	**5**	**7**
empirical formula	$C_{38}H_{72}Cl_8F_{18}N_2O_{18}S_6W_6$	$C_{38}H_{72}Cl_8N_8S_6W_6$	$C_{38}H_{72}Cl_8N_8O_6W_6$
formula weight	2766.04	2220.12	2123.76
crystal system	monoclinic	monoclinic	triclinic
space group	$P2_1/c$ (#14)	$P2_1/n$ (#14)	$P\bar{1}$ (#2)
a, Å	11.116(5)	11.3323(9)	11.8009(8)
b, Å	27.952(13)	12.3404(9)	11.9332(8)
c, Å	24.516(11)	44.583(3)	11.9522(8)
α			77.9040(10)
β, deg	95.182(9)	97.089(1)	78.4990(10)
γ			62.5740(10)
V, Å^3	7586.3(5)	6187.1(7)	1450.5(2)
Z	4	4	1
ρ_{calcd}, g/cm^3	2.422	2.383	2.431
μ, cm^{-1} (Mo Kα)	96.19	117.05	122.75
radiation	Mo Kα ($\lambda = 0.71069$ Å)	Mo Kα ($\lambda = 0.71069$ Å)	Mo Kα ($\lambda = 0.71069$ Å)
T, °C	−120	−120	−120
$R(F)^a$	0.043	0.057	0.042
$R_w(F)^b$	0.086	0.114	0.051

^{a} $R(F) = [\sum(|F_o| - |F_c|)|/\sum|F_o|]$. ^{b} $R_w(F) = [\sum w(|F_o| - |F_c|)^2/\sum w|F_o|^2]^{1/2}$. $w = 4F_o^2/\sigma^2(F_o^2)$.

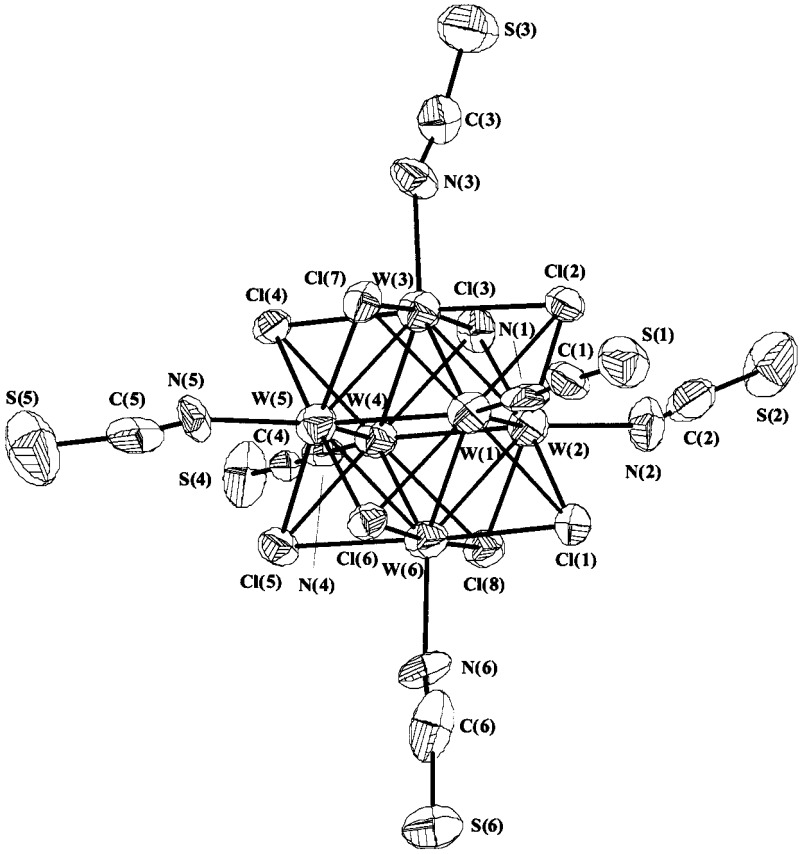

Figure 2. ORTEP diagram of the cluster anion of $[Bu_4N]_2[W_6Cl_8(NCS)_6]$ (**5**). Thermal ellipsoids are drawn at 50% probability.

in energy from 1036 cm^{-1} in $NaOSO_2CF_3$ to 988 cm^{-1}. Additional bands observed in the IR spectra of **1** in Nujol mull, such as the shoulder at 1182 cm^{-1}, likely result from different environments experienced by the triflate ligand. Both the asymmetric and symmetric SO_3 bands appear at energies nearly identical to that of **9**. The IR spectrum of **1** in CH_2Cl_2 also closely resembles that of **9** (Table 1).

An ORTEP diagram of the cluster anion of **1** is shown in Figure 1, crystallographic data are summarized in Table 2, and selected bond distances and angles are summarized in Table 3. The structure of the cluster core $\{W_6Cl_8\}^{4+}$ resembles that of similar clusters previously reported. The average W−W bond length is 2.606 Å, and the average W−Cl bond length is 2.504 Å. Both of these values are comparable with those of other octahedral tungsten clusters containing face-capping chloride ligands.[9,43−46] The average W−O distance of 2.113 Å is similar to the Mo−O distance in **9**,[27] as well as other complexes with a triflate ligand coordinated to a transition metal through one

(43) Mattes, R. *Z. Anorg. Allg. Chem.* **1968**, *357*, 30−42.
(44) Saito, T.; Manabe, H.; Yamagata, T.; Imoto, H. *Inorg. Chem.* **1987**, *26*, 1362−1365.
(45) Healy, P. C.; Kepert, D. L.; Taylor, D.; White, A. H. *J. Chem. Soc., Dalton Trans.* **1973**, 646−650.
(46) Stallmann, M.; Preetz, W. *Z. Anorg. Allg. Chem.* **1999**, *625*, 567−571.

Table 3. Selected Bond Distances and Angles for $[Bu_4N_2]_2[W_6Cl_8(OSO_2CF_3)_6]$ (**1**)

W(1)−W(2)	2.609(1)	W(3)−Cl(3)	2.509(5)
W(1)−W(3)	2.609(2)	W(3)−Cl(6)	2.494(4)
W(1)−W(5)	2.609(1)	W(3)−Cl(8)	2.517(5)
W(1)−W(6)	2.612(1)	W(4)−Cl(3)	2.503(5)
W(2)−W(3)	2.599(2)	W(4)−Cl(4)	2.498(5)
W(2)−W(4)	2.607(2)	W(4)−Cl(7)	2.490(5)
W(2)−W(6)	2.606(2)	W(4)−Cl(8)	2.515(5)
W(3)−W(4)	2.605(1)	W(5)−Cl(3)	2.512(4)
W(3)−W(5)	2.601(2)	W(5)−Cl(4)	2.504(5)
W(4)−W(5)	2.612(1)	W(5)−Cl(5)	2.511(5)
W(4)−W(6)	2.610(2)	W(5)−Cl(6)	2.481(5)
W(5)−W(6)	2.600(2)	W(6)−Cl(1)	2.511(5)
W(1)−Cl(1)	2.500(5)	W(6)−Cl(4)	2.533(5)
W(1)−Cl(2)	2.504(5)	W(6)−Cl(5)	2.515(4)
W(1)−Cl(5)	2.499(5)	W(6)−Cl(7)	2.488(5)
W(1)−Cl(6)	2.483(5)	W(1)−O(1)	2.12(1)
W(2)−Cl(1)	2.503(5)	W(2)−O(4)	2.12(1)
W(2)−Cl(2)	2.502(5)	W(3)−O(7)	2.12(1)
W(2)−Cl(7)	2.495(5)	W(4)−O(10)	2.11(1)
W(2)−Cl(8)	2.504(5)	W(5)−O(13)	2.11(1)
W(3)−Cl(2)	2.515(5)	W(6)−O(16)	2.07(1)
W(1)−O(1)−S(1)	138.3(7)	W(4)−O(10)−S(4)	138.4(8)
W(2)−O(4)−S(2)	137.0(8)	W(5)−O(13)−S(5)	133.9(7)
W(3)−O(7)−S(3)	133.1(7)	W(6)−O(16)−S(6)	137.3(7)

oxygen atom.[47] The W−W−W bond angles are very close to the expected values of 60° and 90°. In contrast to the structures of $[BzMe_3N]_2[Mo_6Cl_8(OSO_2CF_3)_6]$,[27] $[Bu_4N]_2[Ta_6Cl_{12}(OSO_2CF_3)_6]$,[29] and $[Bu_4N]_3[Nb_6Cl_{12}(OSO_2CF_3)_6]$,[30] there is no disorder for the triflate ligands in compound **1**. The triflate ligands in the cluster $[Ph_4P]_2[W_6I_8(OSO_2CF_3)_6]$ were not reported to be disordered.[32]

The triflate cluster **1** is an effective precursor for the preparation of clusters with variety of axial ligands. The clusters **2**−**8** have been prepared from **1**. Yields for clusters with halides in the axial positions are relatively high, while those with pseudohalides in the axial positions are significantly lower, because **1** is unstable in alcoholic solvents, which limits its substitution chemistry relative to that of **9**. The molybdenum triflate cluster has been converted to $Na_2[Mo_6Cl_8(OMe)_6]$ (**10**),[27] which has been used in reactions with Bronsted acids HA to provide a variety of substitution products.[48] However, all attempts to prepare the tungsten analogue of **10** resulted in intractable products.

Cluster **1** decomposes more readily in reactions with basic ligands, such as acetate, azide, and methoxide, than in reactions with less basic ligands, such as cyanate, thiocyanate, and selenocyanate. Reaction of **1** with tetrabutylammonium acetate in CH_2Cl_2 or sodium azide in methanol resulted in intractable products. Because azide and acetate are the most strongly basic anions that were reacted with **1**, it appears that ligands with a pK_a value for their corresponding acid greater than approximately 4.5 cause decomposition of **1**.

FAB mass spectrometry has been found to be useful in determining the nature of the products derived from substitution of the triflate ligands in **1**. FAB mass spectral data is summarized in Table 4 for the clusters **1**−**8**. The three highest mass envelopes are assigned to the parent ion plus one cation, the parent ion, and the parent ion minus one ligand. The mass envelope of the parent ion corresponds to the expected isotopic distribution. The *R* factor, which is analogous to the crystallographic *R* factor, has been determined for the parent ion mass envelopes. This provide a measure of the fit of the observed mass envelope to a theoretical one, and an *R* factor less than 5% corresponds to an excellent fit.

Table 4. FAB Mass Spectrometry Data for the Metal Clusters **1**−**9** and Their Ion Pairs

species	mass (highest intensity) calcd	obs	rel intens	*R*, %
$[Bu_4N][W_6Cl_8(OSO_2CF_3)_6]^-$	2523	2521	1.00	3.52
$[W_6Cl_8(OSO_2CF_3)_6]^-$	2281	2282	0.45	2.54
$[W_6Cl_8(OSO_2CF_3)_5]^-$	2132	2131	0.50	2.97
$[Bu_4N][W_6Cl_8Cl_6]^-$	1841	1841	0.20	1.25
$[W_6Cl_8Cl_6]^-$	1599	1599	1.00	1.36
$[W_6Cl_8Cl_5]^-$	1564	1564	0.53	1.87
$[Bu_4N][W_6Cl_8Br_6]^-$	2108	2106	0.40	3.88
$[W_6Cl_8Br_6]^-$	1866	1866	1.00	1.52
$[W_6Cl_8Br_5]^-$	1786	1786	0.58	1.63
$[W_6Cl_8I_6]^-$	2148	2148	1.00	2.41
$[W_6Cl_8I_5]^-$	2018	2020	0.93	5.07
$[Bu_4N][W_6Cl_8(NCS)_6]^-$	1977	1977	1.00	2.38
$[W_6Cl_8(NCS)_6]^-$	1735	1735	0.74	2.11
$[W_6Cl_8(NCS)_5]^-$	1677	1677	0.23	4.71
$[Bu_4N][W_6Cl_8(NCSe)_6]^-$	2259	2260	1.00	4.95
$[W_6Cl_8(NCSe)_6]^-$	2016	2016	0.68	1.72
$[W_6Cl_8(NCSe)_5]^-$	1912	1912	0.31	5.41
$[Bu_4N][W_6Cl_8(NCO)_6]^-$	1881	1881	1.00	1.26
$[W_6Cl_8(NCO)_6]^-$	1639	1640	0.63	3.29
$[W_6Cl_8(NCO)_5]^-$	1597	1596	0.32	3.85
$[W_6Cl_8(O{=}PPh_3)_3][OSO_2CF_3]_3^+$	2669	2673	1.00	6.52

Table 5. Characteristic IR Frequencies for $[W_6Cl_8L_6]^n$, $n = 2-$ or $4+$[a]

species	infrared band, cm^{-1}	assignment
$[Bu_4N]_2[W_6Cl_8(NCO)_6]$	2217	ν(CN)
$[Bu_4N]_2[W_6Cl_8(NCS)_6]$	2047	ν(CN)
$[Bu_4N]_2[W_6Cl_8(NCSe)_6]$	2042	ν(CN)
$[W_6Cl_8(O{=}PPh_3)_6][OSO_2CF_3]_4$	1063	ν(PO)

[a] In CH_2Cl_2.

Several of the products obtained from **1** have IR bands which shift upon coordination of the ligand, as summarized in Table 5. The triphenylphosphine oxide complex **8** has a ν(P═O) stretching band at 1063 cm^{-1}, which is shifted to lower energy relative to the ν(P═O) band at 1189 cm^{-1} of free triphenylphosphine oxide. The ν(CN) band of the thiocyanate cluster **5** is lowered in energy relative to free thiocyanate, from 2053 cm^{-1} in KSCN to 2047 cm^{-1} in **5**, which can be attributed to N-bonding of the ligand to tungsten.[49] The ν(CN) band in **6** is also shifts from 2072 cm^{-1} in KNCSe to 2042 cm^{-1} in **6**, indicating that the selenocyanate ligand is also bound to tungsten through the nitrogen atom. The cyanate cluster **7** exhibits an increase in the energy of the ν(CN) band, from 2162 cm^{-1} in NaNCO to 2217 cm^{-1} in the cluster, which is indicative of N-bonding, as observed in a variety of other cyanate complexes.[50]

To investigate the ligand disposition in clusters **5** and **7**, X-ray crystal structures were obtained. An ORTEP diagram for the cluster anion of **5** is shown in Figure 2, a packing diagram is shown in Figure 3, and an ORTEP diagram for the cluster anion of **7** is shown in Figure 4. Crystallographic data are summarized in Table 2, and selected bond lengths and angles are presented in Tables 6 (**5**) and 7 (**7**). The structure of the anion of **5** resembles that of $[(Ph_3P)_2N]_2[W_6Cl_8(NCS)_6]$ (**11**).[46] As indicated by IR spectroscopy, all thiocyanate ligands in **5** are bound though the nitrogen atoms. The structure of the $\{W_6Cl_8\}^{4+}$ core

(47) Lawrence, G. A. *Chem. Rev.* **1986**, *86*, 17−33.
(48) Prokopuk, N. Ph.D. Thesis, Northwestern University, Evanston, IL, 1998.
(49) Weissenhorn, R. G. *Z. Anorg. Allg. Chem.* **1976**, *426*, 159−172.
(50) Nakamoto, K. *Infrared and Raman Spectra of Inorganic and Coordination Compounds*, 3rd ed.; John Wiley & Sons: New York, 1978.

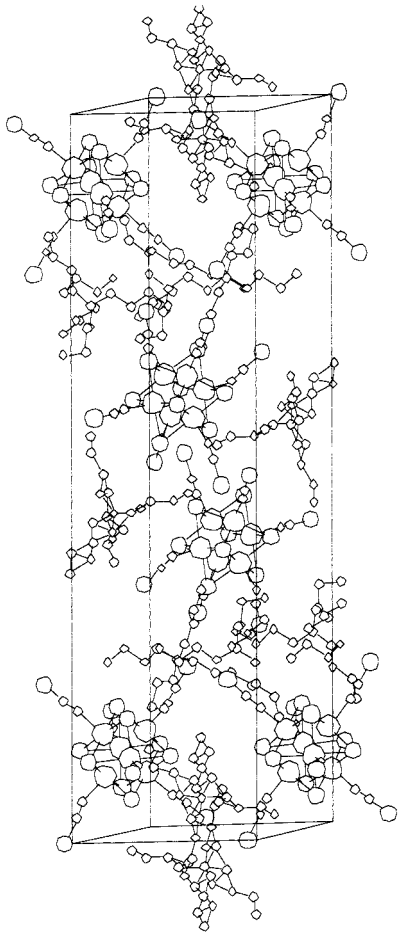

Figure 3. Packing diagram for $[Bu_4N]_2[W_6Cl_8(NCS)_6]$ (**5**).

in **5** very similar to that of **11**. However, the W−N bond lengths in **5** range from 2.09 to 2.15 Å, with an average value of 2.12 Å, which is slightly longer than the average W−N bond length of 2.097 Å reported for **11**. The W−N−C and N−C−S angles of **5** range from 151.6° to 172.7° (average value = 159.6°) and 168.6° to 174.5° (average value = 172.7°), respectively. While the W−N−C bonds in **11** are nearly linear, with an average angle of 174.4°, those of **5** are more sharply bent. The bent W−N−C angles in **5** may be induced by crystal packing forces exerted by the $[Bu_4N]^+$ cation, relative to the more rigid $[(Ph_3P)_2N]^+$ cation.

The structure of **7** shows that the cyanate ligand is bound to the tungsten centers through the nitrogen atom. The cluster core of **7** again resembles that of previously characterized examples.[9,43−46] The W−N−C bonds in **7** are bent with an average angle of 162.7°, while the NCO^- ligand is nearly linear, with an average N−C−O bond angle of 177.3°. The CN bonds in **7** are short (average value = 1.16 Å), indicative of a triple CN bond, which would be expected in this binding mode. The bonding of the NCO^- ligand in **7** is identical to that in $[Bu_4N]_2[Mo_6Cl_8(NCO)_6]$, which was prepared by the reaction of $[Bu_4N]_2[Mo_6Cl_8I_6]$ with AgNCO, where the ligands are bound to molybdenum exclusively though the nitrogen atom.[21]

The ^{13}C and ^{31}P NMR chemical shift values of these species also vary between the free and coordinated ligands. The ^{13}C NMR in CD_2Cl_2 spectra for the pseudohalide clusters **5**−**7** contain singlets at 159 (**5**), 181 (**6**), and 140 (**7**) ppm. These resonances are shifted downfield from those of the free ligands, which occur (in acetone-d_6) at 133 ppm for KSCN, 132 ppm for NaNCO, and 120 ppm for KNCSe. A singlet is found in the ^{31}P NMR spectrum of **8** at 56.2 ppm, which is shifted downfield from the 30.0 ppm resonance of free $O{=}PPh_3$. The NMR spectra indicate a net deshielding of the carbon or phosphorus nuclei upon coordination of the ligands to the tungsten atoms, resulting from a removal of electron density from the ligand by the cluster.

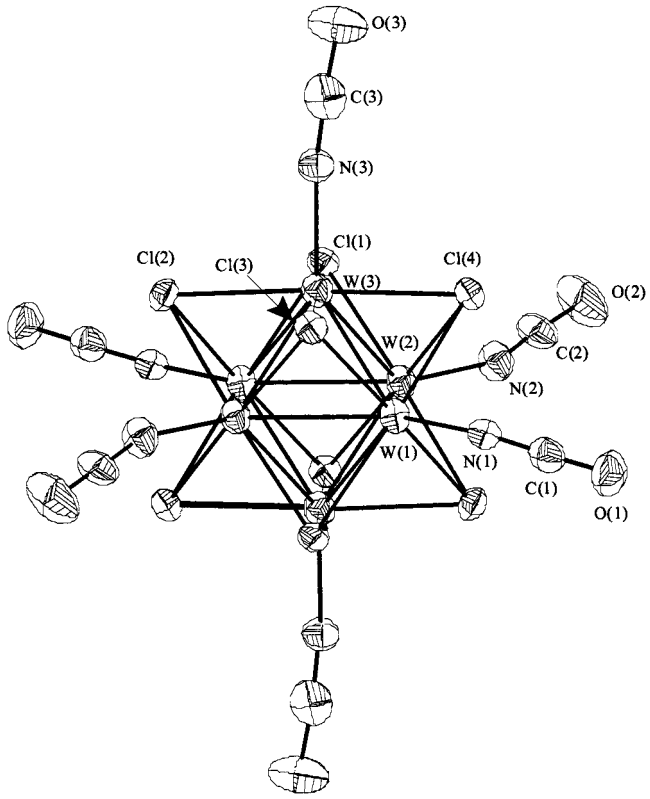

Figure 4. ORTEP diagram of the cluster anion of $[Bu_4N]_2[W_6Cl_8(NCO)_6]$ (**7**).

Table 6. Bond Distances (in Å) and Angles (in deg) for $[Bu_4N_2]_2[W_6Cl_8(NCS)_6]$ (**5**)

W(1)−N(1)	2.12(3)	W(1)−N(1)−C(1)	165.0(3)
W(2)−N(2)	2.09(3)	W(2)−N(2)−C(2)	152.3(4)
W(3)−N(3)	2.15(3)	W(3)−N(3)−C(3)	151.6(3)
W(4)−N(4)	2.12(3)	W(4)−N(4)−C(4)	172.7(2)
W(5)−N(5)	2.14(3)	W(5)−N(5)−C(5)	155.9(4)
W(6)−N(6)	2.11(3)	W(6)−N(6)−C(6)	160.3(4)
N(1)−C(1)	1.13(4)	N(1)−C(1)−S(1)	174.5(4)
N(2)−C(2)	1.09(4)	N(2)−C(2)−S(2)	173.2(4)
N(3)−C(3)	1.10(4)	N(3)−C(3)−S(3)	173.7(4)
N(4)−C(4)	1.20(3)	N(4)−C(4)−S(4)	173.5(3)
N(5)−C(5)	0.99(4)	N(5)−C(5)−S(5)	168.6(4)
N(6)−C(6)	1.00(4)	N(6)−C(6)−S(6)	172.8(4)
C(1)−S(1)	1.62(4)		
C(2)−S(2)	1.73(4)		
C(3)−S(3)	1.64(4)		
C(4)−S(4)	1.55(3)		
C(5)−S(5)	1.71(4)		
C(6)−S(6)	1.77(5)		

Table 7. Selected Bond Distances (in Å) and Angles (in deg) for $[Bu_4N_2]_2[W_6Cl_8(NCO)_6]$ (**7**)

W(1)−N(1)	2.104(9)	W(1)−N(1)−C(1)	157.5(8)
W(2)−N(2)	2.129(8)	W(2)−N(2)−C(2)	162.6(9)
W(3)−N(3)	2.102(8)	W(3)−N(3)−C(3)	168.1(9)
N(1)−C(1)	1.183(13)	N(1)−C(1)−O(1)	175.6(12)
N(2)−C(2)	1.1145(12)	N(2)−C(2)−O(2)	178.3(14)
N(3)−C(3)	1.150(10)	N(3)−C(3)−O(3)	177.9(14)
C(1)−O(1)	1.203(13)		
C(2)−O(2)	1.177(11)		
C(3)−O(3)	1.210(13)		

In conclusion, the hexatriflate cluster compound **1** serves as an effective precursor for the preparation of a variety of axially substituted clusters containing the $\{W_6Cl_8\}^{4+}$ core. Clusters with halide and pseudohalide axial ligands have been prepared from **1** and have been characterized by a variety of analytical techniques. This chemistry should be generally useful for the preparation of clusters of the type $[W_6Q_8L_6]^{n+/n-}$, where Q is a chalcogenide atom, and it may aid the preparation of tungsten analogues to the Chevrel phases.

Acknowledgment. Support from the National Science Foundation award CHE-9417250 is appreciated.

Supporting Information Available: Listings of atomic coordinates, thermal parameters, bond lengths, and bond angles for **1**, **5**, and **7** (not available in cif format). This material is available free of charge via the Internet at http://pubs.acs.org.

IC990791+